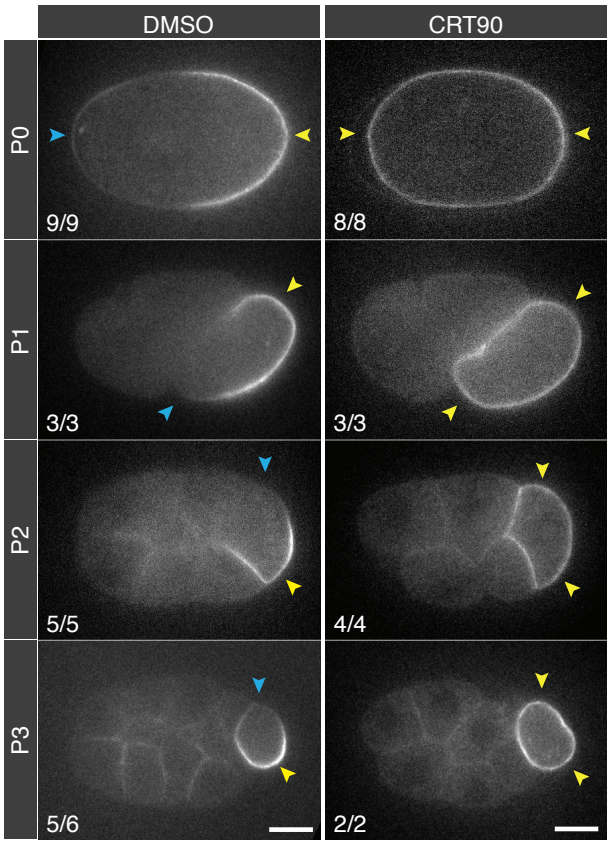

Supplementary Figure S1. Polarisation of P lineage blastomeres P1-P3 requires PKC-3 activity. PAR-2 localisation remains polarized in P lineage cells treated with DMSO, but becomes symmetric upon treatment with the PKC-3 inhibitor CRT90. The fraction of embryos (n/N) undergoing an asymmetric (DMSO) or symmetric division (CRT90) is indicated for each condition. Cyan/yellow arrowhead pairs indicate polarized PAR-2 in control P lineage cells, while yellow arrowhead pairs highlight symmetric distribution of PAR-2 in P lineage cells upon CRT90-treatment. P0 images from dataset in [32] shown for comparison.

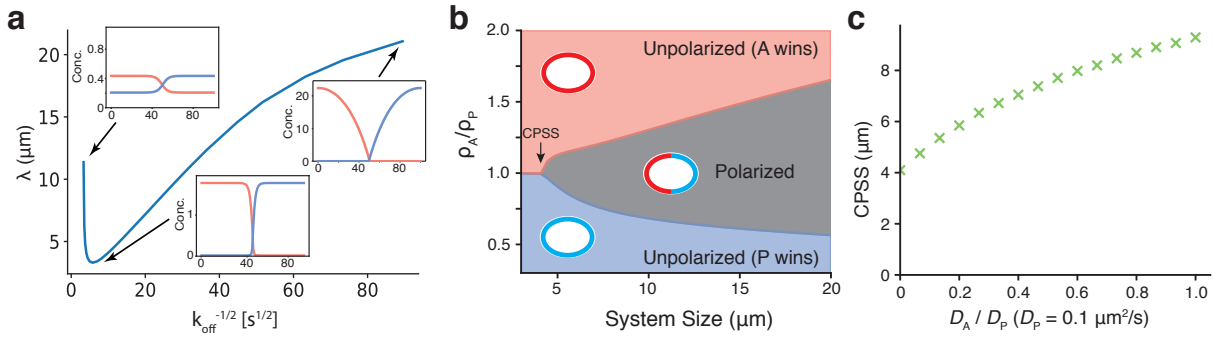

Supplementary Figure S2. The effects of changes to k_{off} alone or unequal diffusion rates in the PAR model. **(a)** Gradient length λ as a function of $\sqrt{1/k_{\text{off}}}$ for the PAR system. Note, in contrast to the case of scaling all reaction rates together as shown in Figure 1F, here the relationship between λ and $\sqrt{1/k_{\text{off}}}$ is non-linear due to the fact that gradient shape changes substantially. This is at least in part due to changes in the balance of material between membrane and cytoplasm - note the vastly different membrane concentrations of PAR species across different values of k_{off}. There is a roughly linear regime for values of $\sqrt{1/k_{\text{off}}}$ between 10 and 50 $\text{s}^{1/2}$. For $\sqrt{1/k_{\text{off}}} < 10$ $\text{s}^{1/2}$, high off rates reduce membrane concentrations below their ability to antagonize each other, allowing them to invade each other's domains. Though this eventually destabilizes polarity completely, this change in shape initially results in increasing λ. For $\sqrt{1/k_{\text{off}}} > 50$ $\text{s}^{1/2}$, the gradient also changes shape as concentrations rise, effectively sharpening one side of the gradient. Boundary effects likely also come into play. **(b)** PAR polarity for asymmetric diffusion coefficients $D_A = 0.0$ $\mu\text{m}^2/\text{s}$, $D_P = 0.1$ $\mu\text{m}^2/\text{s}$. Note the parameter space is distorted, but retains the topology of Figure 1I. **(c)** Effect of varying ratios of D_A/D_P on CPSS, demonstrating the limited effect of changes in D_A so long as D_P is kept constant at 0.1 $\mu\text{m}^2/s$.

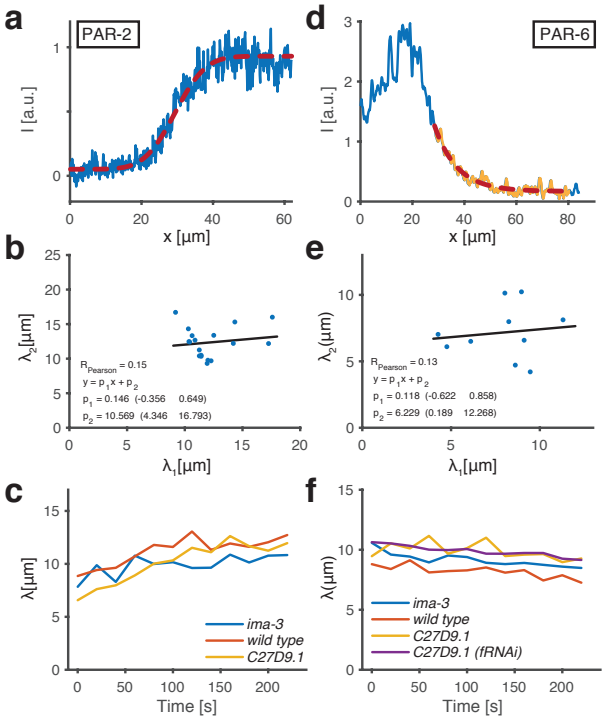

Supplementary Figure S3. Additional information on boundary measurements. **(a)** Sample experimental PAR-2 distribution from anterior to posterior and the corresponding sigma function fit. **(b)** Plotting the length scale of the two interface width measurements λ_1, λ_2 obtained for PAR-2 in each embryo image revealed no correlation and hence can be considered independent (see Methods). Each data point marks an individual embryo. Data points were obtained as nanmean() from three consecutive timepoints prior to cytokinesis (see methods). Embryos that yielded no gradient for one of the two sides were discarded for this graph. **(c)** Plot of mean interface width λ for PAR-2 as a function of time before cytokinesis onset in P0. Interface width shows sharpening beginning around two minutes prior to cytokinesis onset. **(d)** Sample experimental PAR-6 distribution from anterior to posterior and the corresponding exponential fit. This difference in shape between PAR-2 and PAR-6 is consistent with evidence that distinct molecular mechanisms may be involved in maintaining asymmetry of anterior and posterior PAR proteins [22, 32, 34, 53, 54]. **(e)** Same as (b), but for PAR-6. **(f)** Plot of mean interface width λ for PAR-6 as a function of time before cytokinesis onset in P0. Note interface width is generally constant, increasing only slightly in the period prior to cytokinesis onset.

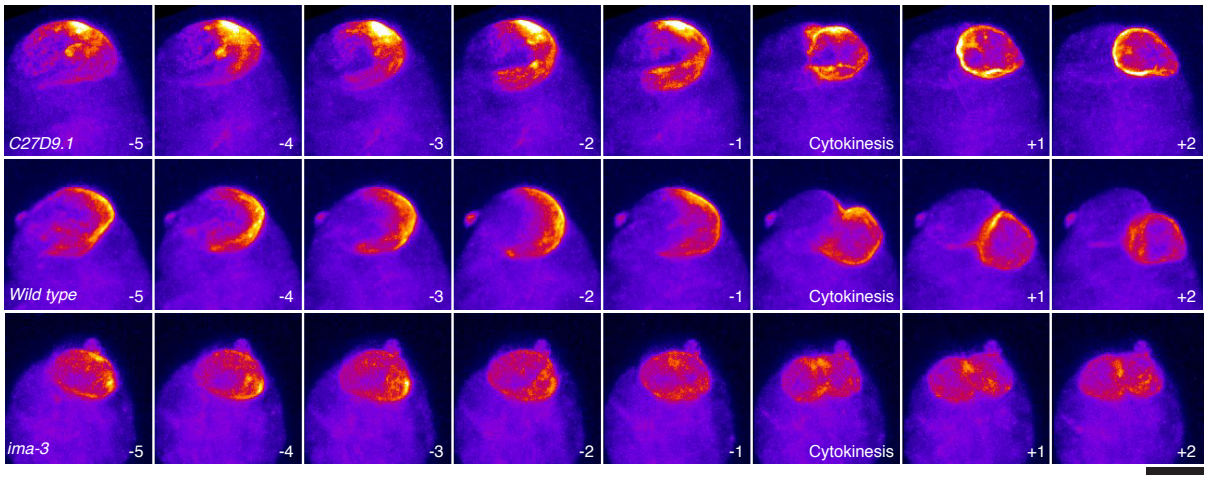

Supplementary Figure S4. Full timeseries of different sized P3 cells undergoing cytokinesis. Full timeseries of wild-type, *C27D9.1*, and *ima-3* embryos expressing GFP::PAR-2 shown in Figure 5e. Time (minutes) is shown relative to cytokinesis. Scale bar, 5 µm. Full asymmetry data set provided in Supplementary Table S1.

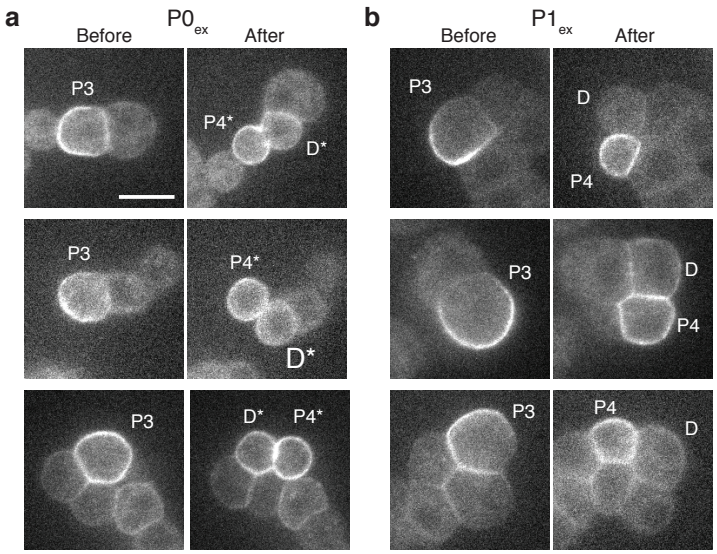

Supplementary Figure S5. Additional examples of P3 divisions in $P0_{ex}$ and $P1_{ex}$. **(a)** Three examples of divisions of P3 cells derived from $P0_{ex}$ cells expressing PAR-2::GFP. P3 is shown prior to division on the left and the P3 daughters, D and P4, on the right. Note D* and P4* notation are used due to uncertainty in fate. P4* is used to denote the cell closer to E descendants. **(b)** Same as **(a)** but for P3 cells derived from $P1_{ex}$ cells. Scale bar, 10 µm.

Condition	Strain	Date	Embryo	Division Timing, Relative			P3		P3 Daughter Asymmetry	
				E→C	E→P3	C→P3	Circumference	Histogram Overlap	Volume	PAR-2
C26D9.1	NWG0025	23/08/2017	1	nc	nc	6	51	0.37	0.71	0.50
			3	4	9	5	54	0.1	0.79	0.83
		24/08/2017	1	2	8	6	52	0.31	0.85	0.76
			2	8	10	2	52	0.13	0.93	0.80
			3	7	10	3	50	0.15	1.01	0.77
wild type	NWG0079	22/07/2017	1	4	14	10	50	0.05	1.04	0.88
			2	nc	nc	8	49	0.39	0.65	0.53
		10/08/2017	2	2	13	11	49	0.19	0.73	0.69
		06/09/2017	1	4	11	7	50	0.18	1.12	0.88
			3	5	13	8	48	0.07	1.23	0.85
		07/09/2017	1	4	11	7	47	0.05	1.12	0.84
			2	3	13	10	49	0.26	1.12	0.71
ima-3	TH120	17/08/2017	1	6	18	12	41	0.48	0.17	0.51
			2	9	21	12	44	0.32	0.36	0.47
			3	nc	nc	nc	43	0.54	0.22	0.25
		15/08/2017	1	7	17	10	44	0.42	0.36	0.51
			3	5	25	16	41	0.55	0.05	0.36
		14/08/2017	1	10	23	13	42	0.64	0.37	0.21
			3	10	25	15	40	0.63	0.18	0.31
	NWG0079	11/08/2017	1	unclear	unclear	unclear	37	0.6	0.06	0.12
		08/08/2017	1	10	29	19	43	0.5	0.08	0.16
			2	nc	nc	nc	41	0.69	0.26	0.10
			3	22	16	-6	40	0.77	0.58	0.59
		21/12/2017	1	6	16	10	39	0.36	0.36	0.56

nc - Relevant timepoints not captured; unclear - E/C identities could not be clearly established.

Supplementary Table S1. Division timings and asymmetries for P3 cells from different-sized embryos.

C. elegans Strain	Genotype	Source
KK1228	*pkc-3(it309 [gfp::pkc-3]) II*	CGC
KK1248	*par-6(it310[par-6::gfp]) I*	CGC
KK1273	*par-2 (it328[gfp::par-2])*	CGC
N2	Wild type	CGC
NWG0025	*C27D9.1(tm5009) unc-119(ed3) III; ddIs26[mCherry::T26E3.3 (par-6) + unc-119(+)]; ddIs25[pie-1::gfp::par-2[RNAi res. SacI/MluI])b + unc-119]*	This work
NWG0026	*unc-119 (ed3) III; ddIs31[pie-1p::mCherry::par-2;unc-119(+)]; par-6(it310[par-6::gfp]) I*	[32]
NWG0055	*unc-119(ed3)III; ddIs26[mCherry::T26E3.3;unc-199(+)]; par-6(it310[par-6::gfp]) I*	This work
NWG0061	*C27D9.1(tm5009) unc-119(ed3)III; ddIs8[pie-1p::GFP::par-6(cDNA)]; ddIs31[pie-1p::mCherry::par-2;unc-119(+)]*	This work
NWG0079	*unc-119(ed3) III; ltIs44pAA173; [pie-1p-mCherry::PH(PLC1δ1) +unc-119(+)] V.; ddIs25[gfp::F58B6.3;unc-119(+)]*	This work
OD58	*unc-119(ed3) III; ltIs38[pAA1; pie-1::gfp::PH(PLC1δ1) + unc-119(+)].*	[55]
TH120	*unc-119(ed3) III; ddIs25; ddIs26[mCherry::T26E3.3 (par-6) + unc-119(+)]*	[56]
TH129	*unc-119(ed3) III; ddIs25[pie-1::gfp::par-2[RNAi res. SacI/MluI])b + unc-119]*	[56]
TH411	*unc-119(ed3)III; ddIs8[pie-1p::gfp::par-6(cDNA); ddIs31[pie-1p::mCherry::par-2;unc-119(+)]*	[7]

Supplementary Table S2. Worm strains used in this work.

Strain	Source	Typical Time
Feeding RNAi: *control*	[32]	Matched to experiment
Feeding RNAi: *C27D9.1*	Source Bioscience (Ahringer Library)	~36 hrs
Feeding RNAi: *ima-3*	Source Bioscience (Ahringer Library)	20 hrs
Feeding RNAi: *XFP*	C. Eckmann	6-20 hrs

Supplementary Table S3. RNAi feeding clones used in this work.

Supplementary Movie Legends

Supplementary Movie S1. Time evolution of the symmetric PAR model for four points in parameter space from Figure 2d, representing 2% changes in the ratios of total A to P (ρ_A/ρ_P) for $L < \mathrm{CPSS}$ (left) and $L > \mathrm{CPSS}$ (right) as indicated. Note that the system is unstable and breaks down even for small changes in ρ_A/ρ_P below $L > \mathrm{CPSS}$.

Supplementary Movie S2. Timelapse video of an embryo expressing mCherry::PH-PLCδ1 (cyan) and GFP::PAR-2 (red) imaged by diSPIM from the zygote stage through division of P4. P lineage cells are easily distinguished by the presence of PAR-2 which is segregated asymmetrically in each of the first 4 divisions. P4 moves away from the objective after its birth, obscuring its visibility. Maximum Z projection shown. Scale bar, 10 µm. Time (hh::mm).

Supplementary Movie S3. Timelapse videos capturing P3 division in *C27D9.1* (top) and *ima-3* (bottom) embryos expressing GFP::PAR-2. Maximum Z projection shown. Scale bar, 10 µm. Time (mins) relative to cytokinesis.

Supplementary Movie S4. Timelapse videos of dissected $P0_{ex}$ (left) and $P1_{ex}$ (right) cells from GFP::PAR-2 labeled embryos as shown in Figure 6e,f. Elapsed time (hh:mm:ss) shown. Variable intervals used to allow capture of key events in both cells on the same slide. P3 birth and division noted by arrows. Scale bar, 10 µm.